

SPARSE WAVEFORM DESIGN FOR ALL-SPECTRUM CHANNELIZATION

George Sklivanitis,[†] Panos P. Markopoulos,^{*} Stella N. Batalama,[†] and Dimitris A. Pados[†]

[†]Dept. of Electrical Engineering, State University of New York at Buffalo, NY 14260

E-mail: {gsklivan, batalama, pados}@buffalo.edu

^{*}Dept. of Electrical and Microelectronic Engineering, Rochester Institute of Technology, NY 14623

E-mail: panos@rit.edu

ABSTRACT

We introduce maximum-SINR sparse-binary waveforms that modulate data information symbols from any finite alphabet and span the whole continuum of the available/device-accessible spectrum. We offer an optimal algorithm that designs the proposed waveforms by maximizing the signal-to-interference-plus-noise ratio (SINR) at the output of the maximum-SINR linear receiver. In addition, we offer a suboptimal algorithm for the same problem with significantly reduced computational complexity. The post-filtering SINR improvements attained by the proposed waveforms in a single-input single-output (SISO) communication system with colored interference are presented analytically. Simulation studies compare the proposed waveforms with their conventional non-sparse counterparts and demonstrate their superior SINR performance.

Index Terms— All-spectrum, binary code sequences, maximum SINR, sparsity, waveform design.

1. INTRODUCTION

In recent years, adaptively optimized binary code waveforms attracted considerable attention with applications in physical layer security, data hiding, and cognitive radio networking. Recent work in cognitive underlay networking [1–5] considers adaptive code waveform optimization for secondary users that operate concurrently in frequency and time with primary users. Binary code waveforms are designed to span the whole continuum of the available spectrum and are cognitively optimized to maximize the signal-to-interference-plus-noise ratio (SINR) at the output of the secondary receiver.

Recently proposed schemes in the context of overloaded code-division multiple-access (CDMA) systems consider sparsity in non-orthogonal code waveforms to enable low complexity, effective detection of multiple users that communicate simultaneously over a common channel. Toward that end, [6] defines a specific group of sparse code sequences to enable near-optimal, multi-user detection using belief propagation (BP). A statistical-mechanics framework for sparse CDMA in [7] demonstrates that small values of sparsity

provide considerable spectral-efficiency performance improvements, while work in [8] presents a design technique for constructing low-density, sparse code sequences with good distance spectrum properties, that ensure good performance in additive-white-Gaussian noise (AWGN) channels. On the other hand, synthesis of low-density spreading sequences in [9] is conducted on a trial-and-error search basis. Another multiplexing scheme that enjoys low-complexity reception due to sparse spreading is presented in [10].

Binary code waveforms for dense spreading sets have been well studied in terms of total-squared correlation (TSC) bounds and optimal designs [11]. New bounds and optimal designs for minimum TSC quaternary signature sets are derived in [12]. Related work on waveform design for sparse spreading binary sets is very limited. Recent work in [13] considers quadrature amplitude modulation (QAM) and provides a framework for designing sparse spreading code matrices with maximum minimum code distance. Code distance is optimized upon a given factor graph structure to ensure maximum-likelihood (ML), and BP detection performance and reduced complexity.

In this paper, instead of static binary code waveforms we propose for the first time in the literature adaptive design of sparse binary code waveforms that maximize SINR at the output of the maximum-SINR linear filter. In this present work, we provide both an optimal sparsity waveform design algorithm and a suboptimal, computationally efficient, iterative design algorithm. Simulation studies demonstrate post-filtering SINR superiority for particular values of sparsity in a single-input single-output (SISO) communication system that operates in colored interference.

2. SYSTEM MODEL

We consider a single-antenna user transmitting information symbols over a SISO flat-fading channel with N paths. The symbols are drawn from a complex constellation \mathcal{A} of energy E and, traditionally, modulated with a length- L binary code waveform $\mathbf{s} \in \{\pm \frac{1}{\sqrt{L}}\}^L$. The down-converted and pulse-matched received signal vector that corresponds to the i -th

transmitted symbol, $b_i \in \mathcal{A}$, is given by

$$\mathbf{y}_i \triangleq \mathbf{H}\mathbf{s}b_i + \mathbf{i}_i + \mathbf{n}_i \in \mathbb{C}^{L_M \times 1}, \quad (1)$$

where $L_M = L + N - 1$, $\mathbf{H} \in \mathbb{C}^{L_M \times L}$ is the multipath channel matrix, $\mathbf{i}_i \in \mathbb{C}^{L_M \times 1}$ accounts for colored interference with autocorrelation matrix $\mathbf{R}_i \triangleq \mathbb{E}\{\mathbf{i}_i\mathbf{i}_i^H\} \in \mathbb{C}^{L_M \times L_M}$, and $\mathbf{n}_i \sim \mathcal{CN}(\mathbf{0}_{L_M}, \sigma^2\mathbf{I}_{L_M})$ is white Gaussian noise. For any general waveform \mathbf{s} with $\|\mathbf{s}\|_2 = 1$ and given symbol-constellation energy E , transmission energy is given by $\rho(\mathbf{s}) \triangleq E\|\mathbf{s}\|_2^2 = E$. By (1), the autocorrelation matrix of the overall disturbance, $\mathbf{d}_i \triangleq \mathbf{i}_i + \mathbf{n}_i$, is $\mathbf{R}_d \triangleq \mathbb{E}\{\mathbf{d}_i\mathbf{d}_i^H\} = \mathbf{R}_i + \sigma^2\mathbf{I}_{L_M}$ and the linear filter at the receiver that exhibits maximum output SINR can be found to be any scaled version of $\mathbf{w}_{\max\text{-SINR}}(\mathbf{s}) \triangleq \mathbf{R}_d^{-1}\mathbf{H}\mathbf{s}$. The corresponding maximum post-filtering SINR is then found to be $\text{SINR}(\mathbf{s}) \triangleq E \mathbf{s}^\top \mathbf{H}^H \mathbf{R}_d^{-1} \mathbf{H} \mathbf{s}$. That is, posterior to max-SINR filtering, for given \mathbf{R}_d and \mathbf{H} , the SINR is only a function of waveform \mathbf{s} . Traditionally, the transmitter seeks to design and employ a maximum-SINR binary waveform $\hat{\mathbf{s}}$, defined as

$$\hat{\mathbf{s}} \triangleq \underset{\mathbf{s} \in \{\pm \frac{1}{\sqrt{L}}\}^L}{\text{argmax}} \mathbf{s}^\top \mathbf{A} \mathbf{s}, \quad (2)$$

where $\mathbf{A} \triangleq \mathbf{H}^H \mathbf{R}_d^{-1} \mathbf{H}$. The above well-known waveform design problem can be solved optimally by exhaustive evaluation of all 2^L binary vectors $\mathbf{s} \in \{\pm \frac{1}{\sqrt{L}}\}^L$. However, the complexity of the problem in (2) grows exponentially with code-waveform length L . Prior work on optimal and suboptimal algorithms for the design of $\hat{\mathbf{s}}$ can be found in [14–18] and references therein. In this work, we make for the first time in the literature a case for the design and employment of sparse-binary maximum-SINR waveforms.

3. PROPOSED SPARSE WAVEFORM DESIGN

3.1. Problem Formulation

We start with the intuitive remark that, due to chip disturbance correlations, there may be chip-transmission intervals wherein the transmitter should avoid operating. Mathematically, allowing for sparsity in (2), we define the sparse-binary max-SINR-optimal waveform

$$\hat{\mathbf{s}}_s \triangleq \underset{\mathbf{s} \in \{0, \pm \frac{1}{\sqrt{L}}\}^L}{\text{argmax}} \mathbf{s}^\top \mathbf{A} \mathbf{s} \quad (3)$$

and, by extension of the feasibility set, we find, indeed,

$$\text{SINR}(\hat{\mathbf{s}}_s) \geq \text{SINR}(\hat{\mathbf{s}}). \quad (4)$$

In addition, $\rho(\hat{\mathbf{s}}_s) = E\|\hat{\mathbf{s}}_s\|_2^2 = E \frac{\|\hat{\mathbf{s}}_s\|_0}{L} \leq E = \rho(\hat{\mathbf{s}})$, where $\|\cdot\|_0$ returns the number of non-zero entries of its argument.

That is, omitting transmission, optimally, in some of the chip intervals could increase post-filtering SINR and, at the same time, reduce transmission energy. Our second important observation is that $\hat{\mathbf{s}}_s$ may not be the most SINR efficient waveform among those that attain transmission energy $\rho(\hat{\mathbf{s}}_s)$. That is, $\hat{\mathbf{s}}_s$ is not necessarily the maximizer of $\mathbf{s}^\top \mathbf{A} \mathbf{s}$ over $\{\mathbf{s} \in \{0, \pm c\}^L; E c^2 \|\mathbf{s}\|_0 = \rho(\hat{\mathbf{s}}_s), c \in \mathbb{R}\}$.

In view of the above, in this paper we focus on designing max-SINR, optimally-sparse binary waveforms for fixed transmission energy. Specifically, we consider transmission energy fixed to E (equal to that of the max-SINR full binary waveform $\hat{\mathbf{s}}$) and propose waveform design by

$$\tilde{\mathbf{s}} \triangleq \underset{\substack{\mathbf{s} \in \{0, \pm c\}^L \\ c^2 \|\mathbf{s}\|_0 = 1, c \in \mathbb{R}}}{\text{argmax}} \mathbf{s}^\top \mathbf{A} \mathbf{s}. \quad (5)$$

Notice that, indeed, for every element \mathbf{s} in the feasibility set of (5), $\rho(\mathbf{s}) = E c^2 \|\mathbf{s}\|_0 = E$, which implies

$$\rho(\tilde{\mathbf{s}}) = \rho(\hat{\mathbf{s}}). \quad (6)$$

In addition, for any $0 < \alpha \leq 1$, we find

$$\begin{aligned} \max_{\substack{\mathbf{s} \in \{0, \pm c\}^L \\ c^2 \|\mathbf{s}\|_0 = 1, c \in \mathbb{R}}} \mathbf{s}^\top \mathbf{A} \mathbf{s} &= \max_{K \in [L]} \max_{\substack{\mathbf{s} \in \{0, \pm \frac{1}{\sqrt{K}}\}^L \\ \|\mathbf{s}\|_0 = K}} \mathbf{s}^\top \mathbf{A} \mathbf{s} \quad (7) \\ &\geq \max_{K \in [L]} \max_{\substack{\mathbf{s} \in \{0, \pm \frac{1}{\sqrt{K}}\}^L \\ \|\mathbf{s}\|_0 = K}} \alpha \mathbf{s}^\top \mathbf{A} \mathbf{s}, \quad (8) \end{aligned}$$

where $[L] \triangleq \{1, 2, \dots, L\}$. (7)-(8) in turn imply

$$\begin{aligned} \max_{\substack{\mathbf{s} \in \{0, \pm c\}^L \\ c^2 \|\mathbf{s}\|_0 = 1, c \in \mathbb{R}}} \mathbf{s}^\top \mathbf{A} \mathbf{s} &\geq \max_{K \in [L]} \max_{\substack{\mathbf{s} \in \{0, \pm \frac{1}{\sqrt{K}}\}^L \\ \|\mathbf{s}\|_0 = K}} \frac{K}{L} \mathbf{s}^\top \mathbf{A} \mathbf{s} \quad (9) \\ &= \max_{K \in [L]} \max_{\substack{\mathbf{s} \in \{0, \pm \frac{1}{\sqrt{K}}\}^L \\ \|\mathbf{s}\|_0 = K}} \mathbf{s}^\top \mathbf{A} \mathbf{s} = \max_{\mathbf{s} \in \{0, \pm \frac{1}{\sqrt{L}}\}^L} \mathbf{s}^\top \mathbf{A} \mathbf{s}. \quad (10) \end{aligned}$$

From (4) and (9)-(10) we conclude

$$\text{SINR}(\tilde{\mathbf{s}}) \geq \text{SINR}(\hat{\mathbf{s}}). \quad (11)$$

By (6) and (11), the proposed optimal sparse-binary waveform $\tilde{\mathbf{s}}$ attains the same transmission energy with the conventional binary waveform designed per (2), while it offers higher or equal post-filtering SINR.

3.2. Optimal Algorithm

It is clear at this point that the problem in (5) is a combinatorial problem. Therefore, its solution can be found by exhaustive search within its feasibility set. The description of an optimal algorithm for this task follows.

First, we focus on solving the inner maximization problem in (7), for every $K \in \{1, 2, \dots, L\}$, to obtain

$$\tilde{\mathbf{s}}_K \triangleq \underset{\substack{\mathbf{s} \in \{0, \pm \frac{1}{\sqrt{K}}\}^L \\ \|\mathbf{s}\|_0 = K}}{\text{argmax}} \mathbf{s}^\top \mathbf{A} \mathbf{s}. \quad (12)$$

The solution to (12) can be found by examining exhaustively all $\binom{L}{K} 2^K$ elements of its feasibility set. Then, we obtain $\tilde{\mathbf{s}}$ by solving

$$\tilde{\mathbf{s}} = \underset{\mathbf{s} \in \{\tilde{\mathbf{s}}_1, \dots, \tilde{\mathbf{s}}_L\}}{\text{argmax}} \mathbf{s}^\top \mathbf{A} \mathbf{s}. \quad (13)$$

Certainly, (13) can be solved online by updates every time (12) is solved for some K . Therefore, (5) can be solved optimally by means of the presented algorithm by exhaustive search among all

$$\sum_{K=1}^L \binom{L}{K} 2^K = 3^L \quad (14)$$

elements of its feasibility set, with complexity $\mathcal{O}(3^L)$.¹ A pseudocode of the presented algorithm is offered in Fig. 1.

3.3. Suboptimal Iterative Algorithm

The complexity of the optimal algorithm presented above may be prohibitive for real-time application when L is large. In this section, we present a suboptimal iterative algorithm for solving (5) with complexity $\mathcal{O}(L^4)$. We commence our algorithm by decomposing \mathbf{A} —e.g., by means of eigenvalue decomposition (EVD)—as $\mathbf{A} = \mathbf{W}^H \mathbf{W}$, for some $\mathbf{W} \in \mathbb{C}^{L \times L}$. Then, by the Cauchy-Schwarz inequality [20],

$$\max_{\substack{\mathbf{s} \in \{0, \pm \frac{1}{\sqrt{K}}\}^L \\ \|\mathbf{s}\|_0 = K}} \sqrt{\mathbf{s}^\top \mathbf{A} \mathbf{s}} = \max_{\substack{\mathbf{s} \in \{0, \pm \frac{1}{\sqrt{K}}\}^L \\ \|\mathbf{s}\|_0 = K}} \max_{\substack{\mathbf{a} \in \mathbb{C}^L \\ \|\mathbf{a}\|_2 = 1}} \Re\{\mathbf{s}^\top \mathbf{W}^H \mathbf{a}\} \quad (15)$$

$$= \max_{\substack{\mathbf{a} \in \mathbb{C}^L \\ \|\mathbf{a}\|_2 = 1}} \max_{\substack{\mathbf{s} \in \{0, \pm \frac{1}{\sqrt{K}}\}^L \\ \|\mathbf{s}\|_0 = K}} \Re\{\mathbf{s}^\top \mathbf{W}^H \mathbf{a}\}, \quad (16)$$

where $\Re\{\cdot\}$ returns the real part of its argument. For any given \mathbf{s} in the feasibility set of the outer maximization in (15), the inner maximization is achieved for

$$\mathbf{a} = \frac{\mathbf{W} \mathbf{s}}{\|\mathbf{W} \mathbf{s}\|_2}. \quad (17)$$

Also, for any given \mathbf{a} in the feasibility set of the outer maximization in (16), the inner maximization is achieved for

$$\mathbf{s} = \frac{1}{\sqrt{K}} \text{sgn}(\mathcal{I}_K(\Re\{\mathbf{W}^H \mathbf{a}\})), \quad (18)$$

where $\text{sgn}(\cdot)$ returns the sign of its argument (by convention, $\text{sgn}(0) = 0$), and $\mathcal{I}_K(\cdot)$ returns its argument after setting to zero the $L - K$ entries with the lowest absolute values.

¹Equality in (14) holds by the Binomial Theorem [19].

Optimal Algorithm

Input: $\mathbf{A} = \mathbf{H}^H \mathbf{R}_d^{-1} \mathbf{H}$

- 1: $\tilde{\mathbf{s}} \leftarrow \frac{1}{\sqrt{L}} \mathbf{1}_L; m \leftarrow \tilde{\mathbf{s}}^\top \mathbf{A} \tilde{\mathbf{s}}$
- 2: for $K \in \{1, 2, \dots, L\}$
- 3: for $\mathcal{I} \subseteq \{1, 2, \dots, L\}, |\mathcal{I}| = K$
- 4: for $\mathbf{b} \in \{\pm \frac{1}{\sqrt{K}}\}^K$
- 5: $[\mathbf{s}]_{\mathcal{I}} \leftarrow \mathbf{b}, [\mathbf{s}]_{\{1, 2, \dots, L\} \setminus \mathcal{I}} \leftarrow \mathbf{0}_{L-K}$
- 6: if $\mathbf{s}^\top \mathbf{A} \mathbf{s} > m, \tilde{\mathbf{s}} \leftarrow \mathbf{s}, m \leftarrow \tilde{\mathbf{s}}^\top \mathbf{A} \tilde{\mathbf{s}}$

Output: $\tilde{\mathbf{s}}$

Fig. 1. Pseudocode for the presented optimal algorithm that solves (5) to design the proposed optimally-sparse max-SINR waveform.

By the above observations, for every $K \in \{1, 2, \dots, L\}$, the algorithm initializes at some arbitrary $\mathbf{a}_K^{(0)} \in \mathbb{C}^{L \times 1}$ with $\|\mathbf{a}_K^{(0)}\|_2 = 1$ and generates a converging sequence of points in the feasibility set of (12), $\{\mathbf{s}_K^{(t)}\}_{t=1, 2, \dots}$. Specifically, at the t -th iteration step, $t > 1$, the algorithm calculates

$$\mathbf{s}_K^{(t)} = \frac{1}{\sqrt{K}} \text{sgn}\left(\mathcal{I}_K\left(\Re\left\{\mathbf{W}^H \mathbf{a}_K^{(t-1)}\right\}\right)\right), \quad (19)$$

$$\mathbf{a}_K^{(t)} = \frac{\mathbf{W} \mathbf{s}_K^{(t)}}{\|\mathbf{W} \mathbf{s}_K^{(t)}\|_2}. \quad (20)$$

Certainly, $\Re\{\mathbf{s}_K^{(t)} \mathbf{W}^H \mathbf{a}_K^{(t)}\} \geq \Re\{\mathbf{s}_K^{(t-1)} \mathbf{W}^H \mathbf{a}_K^{(t-1)}\}$ and, since $\Re\{\mathbf{s}_K^{(t)} \mathbf{W}^H \mathbf{a}_K^{(t)}\}$ is bounded by (15), the algorithm will converge in a finite number of steps $T_K > 1$. After obtaining a converging point $\mathbf{s}_K \triangleq \mathbf{s}_K^{(T_K)}$ by the above iterations for every $K \in \{1, 2, \dots, L\}$, the algorithm returns the approximate solution to (5)

$$\mathbf{s}_{\text{IT}} \triangleq \underset{\mathbf{s} \in \{\mathbf{s}_1, \mathbf{s}_2, \dots, \mathbf{s}_L\}}{\text{argmax}} \mathbf{s}^\top \mathbf{A} \mathbf{s}. \quad (21)$$

A pseudocode for the presented iterative algorithm is given in Fig. 2. In the sequel we discuss its complexity and present a modification for further performance enhancement.

a) Complexity: Decomposition $\mathbf{A} = \mathbf{W}^H \mathbf{W}$ costs $\mathcal{O}(L^3)$ (e.g., by means of EVD). Then, for every $K \in \{1, 2, \dots, L\}$, the algorithm executes T_K iteration steps. At each iteration step, say the t -th, the cost to find $\mathbf{s}_K^{(t)}$ and $\mathbf{a}_K^{(t)}$ is $\mathcal{O}(L^2)$. Therefore, the cost for all iterations for all values of K is $\mathcal{O}(\sum_{K=1}^L T_K L^2)$. Setting, in practice, $T_K \leq L$, for every K , all iterations cost $\mathcal{O}(L^4)$. Thus, the overall cost of the proposed iterative algorithm is $\mathcal{O}(L^4)$.

b) Modification: The performance of the proposed suboptimal algorithm can be improved if, for each value of K , we run the presented iterations on $P > 1$ distinct (arbitrary) initializations $\mathbf{a}_{K,1}^{(0)}, \dots, \mathbf{a}_{K,P}^{(0)}$, obtaining corresponding converging points $\mathbf{s}_{K,1}, \dots, \mathbf{s}_{K,P}$. Then, we select as \mathbf{s}_K to be

Suboptimal Iterative Algorithm

Input: $\mathbf{A} = \mathbf{H}^H \mathbf{R}_d^{-1} \mathbf{H}$

- 1: calculate $\mathbf{W} \in \mathbb{C}^{L \times L}$ such that $\mathbf{A} = \mathbf{W}^H \mathbf{W}$
- 2: for $K \in \{1, 2, \dots, L\}$
- 3: $\mathbf{a} \leftarrow$ arbitrary in $\mathbb{C}^{L \times 1}$, with $\|\mathbf{a}\|_2 = 1$; $m \leftarrow 0$
- 4: until convergence,
- 5: $\mathbf{s} \leftarrow \frac{1}{\sqrt{K}} \text{sgn}(\mathcal{I}_K(\Re\{\mathbf{W}^H \mathbf{a}\}))$
- 6: $\mathbf{a} \leftarrow \frac{\mathbf{W}\mathbf{s}}{\|\mathbf{W}\mathbf{s}\|_2}$
- 7: $m' \leftarrow \mathbf{s}^T \mathbf{A} \mathbf{s}$
- 8: if $m' - m \leq \text{threshold}$; $\mathbf{s}_K \leftarrow \mathbf{s}$; convergence
- 9: $m \leftarrow m'$
- 11: $\mathbf{s}_{\text{IT}} \leftarrow \text{argmax}_{\mathbf{s} \in \{\mathbf{s}_1, \dots, \mathbf{s}_L\}} \mathbf{s}^T \mathbf{A} \mathbf{s}$

Output: \mathbf{s}_{IT}

Fig. 2. Pseudocode for the presented suboptimal iterative algorithm for solving (5).

examined in (21) the element of $\{\mathbf{s}_{K,1}, \dots, \mathbf{s}_{K,P}\}$ that offers the highest value in the optimization metric of (5). By this modification, the complexity increases to $\mathcal{O}(PL^4)$.

4. SIMULATION STUDIES AND CONCLUSIONS

In this section, we present simulation studies to demonstrate the performance of both the optimal and the suboptimal iterative sparse-binary waveform design algorithms proposed in this work. In all presented studies, we fix $L = 10$, $N = 1$, $\text{Tr}(\mathbf{R}_i) = 25$ dB, $\|\mathbf{H}\|_F = 1$, $\sigma = 1$, and $E = 10$ dB.

In Fig. 3, we consider a single $(\mathbf{H}, \mathbf{R}_d)$ configuration and plot the post-filtering SINR attained by $\tilde{\mathbf{s}}_K$, solution to (12), for $K = 1, 2, \dots, L$. We also plot the SINRs of $\hat{\mathbf{s}}$, solution to (2), and $\tilde{\mathbf{s}}$, solution to (5). We observe that, expectedly, $\text{SINR}(\hat{\mathbf{s}}) = \text{SINR}(\tilde{\mathbf{s}}_L)$. Also, we notice that $\tilde{\mathbf{s}}_1$ attains inferior performance to that of the optimal non-sparse waveform $\hat{\mathbf{s}}$. However, importantly, for every sparsity K from 2 to 9, $\tilde{\mathbf{s}}_K$ outperforms $\hat{\mathbf{s}}$ with a maximum SINR difference for $K = 5$ (i.e., $\tilde{\mathbf{s}} = \tilde{\mathbf{s}}_5$). Fig. 3 is in accordance with our theoretical results in Section 3 and highlights the benefits of sparsity in the employed waveform.

Next, we plot in Fig. 4 the empirical cumulative distribution function (CDF) of the SINR performance degradation percentage (with respect to the proposed sparse-binary optimal $\tilde{\mathbf{s}}$), attained by the conventional optimal non-sparse waveform $\hat{\mathbf{s}}$ and waveform \mathbf{s}_{IT} , calculated by the presented suboptimal algorithm for $P = 1$ and $P = 20$. For any waveform \mathbf{s} with $\|\mathbf{s}\|_2 = 1$, SINR degradation percentage is defined as $\frac{\text{SINR}(\tilde{\mathbf{s}}) - \text{SINR}(\mathbf{s})}{\text{SINR}(\tilde{\mathbf{s}})} \%$. Vertically plotted lines show the average SINR degradation for the three different waveforms (Δ for $\hat{\mathbf{s}}$, ∇ for $\mathbf{s}_{\text{IT}} (P = 1)$, and \times for $\mathbf{s}_{\text{IT}} (P = 20)$). First, it is most interesting to notice the superiority of the proposed sparse-binary waveform $\tilde{\mathbf{s}}$, compared to the conven-

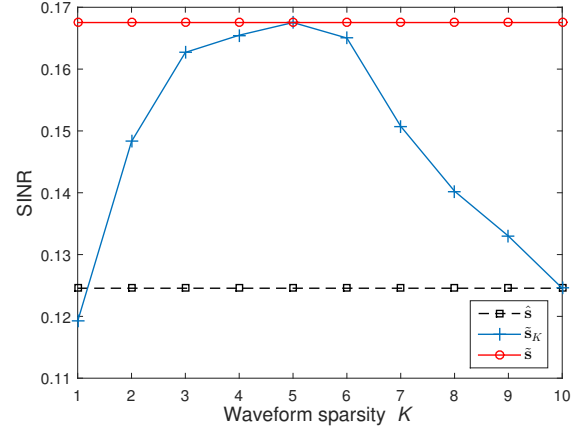


Fig. 3. Maximum post-filtering SINR versus sparsity K .

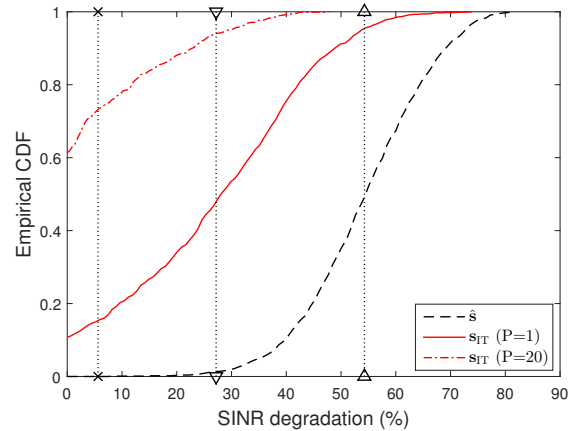


Fig. 4. Empirical CDF of performance degradation attained by $\hat{\mathbf{s}}$ and \mathbf{s}_{IT} with respect to the proposed optimal sparse-binary waveform $\tilde{\mathbf{s}}$.

tional non-sparse $\hat{\mathbf{s}}$. In particular, we observe that $\hat{\mathbf{s}}$ attains at least 20% lower SINR than $\tilde{\mathbf{s}}$ with empirical probability 1 and 54% lower SINR on average. On the other hand, the sparse-binary \mathbf{s}_{IT} , generated by the presented suboptimal algorithm with cost $\mathcal{O}(L^4)$ on $P = 1$ initialization attains average SINR degradation of 28% (almost half of that of the non-sparse optimal $\hat{\mathbf{s}}$). When the number of initializations increases to $P = 20$, the average SINR degradation for \mathbf{s}_{IT} reduces to about 6% (one-ninth of that of $\hat{\mathbf{s}}$). Also, it is worth noticing that, for $P = 20$, \mathbf{s}_{IT} is optimal (equivalent to $\tilde{\mathbf{s}}$) with empirical probability .6.

In conclusion, in this work, we propose, for the first time in the literature, maximum-SINR sparse-binary waveforms and present the first optimal algorithm for their calculation. In addition, we present a significantly faster suboptimal algorithm for the same problem. Our numerical studies demonstrate that the proposed optimal sparse-binary waveforms offer clearly superior SINR performance compared to the conventional non-sparse counterparts.

5. REFERENCES

- [1] K. Gao, S. N. Batalama, D. A. Pados, and J. D. Matyjas, "Cognitive code-division channelization," *IEEE Trans. Wireless Commun.*, vol. 10, pp. 1090–1097, Apr. 2011.
- [2] —, "Cognitive CDMA channelization," in *Proc. IEEE Asilomar Conf. Signals, Syst. and Comput.*, Pacific Grove, CA, Nov. 2009, pp. 672–676.
- [3] G. Sklivanitis, E. Demirors, A. M. Gannon, S. N. Batalama, D. A. Pados, and T. Melodia, "All-spectrum cognitive channelization around narrowband and wideband primary stations," in *Proc. IEEE Global Commun. Conf. (GLOBECOM)*, San Diego, CA, Dec. 2015, pp. 1–7.
- [4] G. Sklivanitis, E. Demirors, S. N. Batalama, D. A. Pados, and T. Melodia, "ROCH: Software-defined radio toolbox for experimental evaluation of all-spectrum cognitive networking," in *Proc. ACM Workshop Software Radio Implem. Forum (SRIF)*, Paris, France, Sep. 2015, pp. 10–10.
- [5] —, "Realizing all-spectrum cognitive networking on a software-defined radio testbed," in *Proc. ACM Workshop Wireless S3*, Paris, France, Sep. 2015, pp. 18–18.
- [6] J. van de Beek and B. M. Popovic, "Multiple access with low-density signatures," in *Proc. IEEE Global Commun. Conf. (GLOBECOM)*, Honolulu, HI, Nov. 2009, pp. 1–6.
- [7] M. Yoshida and T. Tanaka, "Analysis of sparsely-spread CDMA via statistical mechanics," in *Proc. IEEE Int. Symp. Inf. Theory (ISIT)*, Seattle, WA, Jul. 2006, pp. 2378–2382.
- [8] D. Guo and C. Wang, "Multiuser detection of sparsely spread cdma," *IEEE J. Sel. Areas Commun.*, vol. 26, pp. 421–431, Apr. 2008.
- [9] R. Hoshyar, F. P. Wathan, and R. Tafazolli, "Novel low-density signature for synchronous cdma systems over AWGN channel," *IEEE Trans. Signal Process.*, vol. 56, pp. 1616–1626, Apr. 2008.
- [10] H. Nikopour and H. Baligh, "Sparse code multiple access," in *Proc. IEEE Ann. Int. Symp. Personal, Indoor, and Mobile Radio Commun. (PIMRC)*, London, UK, Sep. 2013, pp. 332–336.
- [11] G. N. Karystinos and D. A. Pados, "New bounds on the total squared correlation and optimum design of ds-cdma binary signature sets," *IEEE Trans. Commun.*, vol. 51, pp. 48–51, Jan. 2003.
- [12] M. Li, S. N. Batalama, D. A. Pados, and J. D. Matyjas, "New bounds on the total-squared-correlation of quaternary signature sets and optimal designs," in *Proc. IEEE Global Commun. Conf. (GLOBECOM)*, Honolulu, HI, Nov. 2009, pp. 1–5.
- [13] G. Song, X. Wang, and J. Cheng, "Signature design of sparsely spread CDMA based on superposed constellation distance analysis," *CoRR*, vol. abs/1604.04362, 2016. [Online]. Available: <http://arxiv.org/abs/1604.04362>
- [14] G. N. Karystinos and D. A. Pados, "Rank-2-optimal adaptive design of binary spreading codes," *IEEE Trans. Inf. Theory*, vol. 53, pp. 3075–3080, Sep. 2007.
- [15] G. N. Karystinos and A. P. Liavas, "Efficient computation of the binary vector that maximizes a rank-deficient quadratic form," *IEEE Trans. Inf. Theory*, vol. 56, pp. 3581–3593, Jul. 2010.
- [16] S. Kundu, P. P. Markopoulos, and D. A. Pados, "Fast computation of the L1-principal component of real-valued data," in *Proc. IEEE Int. Conf. Acoust. Speech Signal Process. (ICASSP)*, Florence, Italy, May 2014, pp. 8028–8032.
- [17] P. P. Markopoulos, G. N. Karystinos, and D. A. Pados, "Optimal algorithms for L1-subspace signal processing," *IEEE Trans. Signal Process.*, vol. 62, pp. 5046–5058, Oct. 2014.
- [18] P. P. Markopoulos, "Reduced-rank filtering on L1-norm subspaces," in *Proc. IEEE Sensor Array Multichannel Signal Process. Workshop (SAM)*, Rio de Janeiro, Brazil, Jul. 2016, pp. 1–5.
- [19] G. Arfken and H. Weber, *Mathematical Methods for Physicists*. Cambridge, MA: Elsevier Academic Press, 2005.
- [20] G. H. Golub and C. F. Van Loan, *Matrix Computations (3rd Ed.)*. Baltimore, MD: Johns Hopkins University Press, 1996.